

Globular Clusters at High Redshift

R. G. Carlberg

Department of Astronomy & Astrophysics

University of Toronto, Toronto ON, M5S 3H8 Canada

carlberg@astro.utoronto.ca

ABSTRACT

Globular clusters will be present at high redshifts, near the very beginning of the galaxy formation process. Stellar evolution ensures that they will be much more luminous than today. We show that the redshift distribution at nano-Jansky levels should be very broad, extending up to the redshift of formation. A bracketing range of choices for the redshift of formation, spectral energy evolution models and population density evolution, leads to the conclusion that the sky densities should be around 10^7 per square degree at 1 nJy ($m_{AB} = 31.4$ mag) in bands around 4 microns. Such high sky densities begin to present a confusion problem at these wavelengths to diffraction limited 6m class telescopes. These star-like, low metallicity, clusters will be a significant foreground population for “first light” object searches. On the other hand they are an exceptionally interesting “second light” population in their own right. Depending on the details of galaxy assembly, the clusters will have a noticeable cross-correlation with galaxies on scales of about 20 arcsec, or less, depending on the details of the buildup of galaxy assembly after globular cluster formation. High redshift globular clusters will be an accessible, direct, probe of the earliest stages of the formation of galaxies and the buildup of metals in the universe.

Subject headings: galaxies: clusters: general, galaxies: interactions, galaxies: star clusters, stars: formation

1. Introduction

Globular clusters contain some of the oldest stars in the universe and have long been vital clues to the earliest phases of the star formation in galaxies (Searle & Zinn 1978; Harris 1991; Cote Marzke & West 1998). In our own galaxy the known globular clusters

are very old (VandenBerg 2000) but there is evidence that they can form at lower redshift in suitably extreme conditions, generally associated with merging galaxies (Zepf et al. 1999; Zhang & Fall 1999; Ashman & Zepf 2001; Cen 2001; Larsen et al. 2001). The great age and low metallicity of globular cluster systems indicates that they should be present at very high redshifts and predate the bulk of their eventual host galaxies’ stars.

The exciting prospect is that direct studies of globular cluster formation and evolution will soon become possible. The next generation of optical-infrared telescopes on the ground and in space will have the capability to detect objects at the nano-Jansky level. An estimate of the faint number counts in the optical was undertaken for HST (van den Bergh 1979) but we concentrate on the IR where the redshifts and rise in numbers is much more dramatic. In the 2 to 5 micron bands, the combination of large k-corrections and substantial stellar brightening raises the fluxes from high redshift clusters into the range of 29-32 AB mag. These nanojansky flux levels are within the capabilities expected of future telescopes.

Today’s globular clusters are likely the survivors of a larger population present at the various times of formation (Fall & Rees 1977; Fall & Zhang 2001). If their co-moving density increases by an order of magnitude over those at low redshift then the globular clusters are likely to appear with numbers at a given flux level that are comparable to sub-galactic mass dark matter halos which are the sites of the “first stars” (Couchman & Rees 1986; Haiman & Loeb 1997; Haiman Abel & Madau 2001).

This paper calculates the magnitude limited distribution of the expected numbers, $n(m)$, the redshift distribution, $n(z|m)$, and estimates the angular clustering properties of the globular cluster population relative to their host galaxies. The predictions are made for filter pass bands sufficiently red that Lyman α trough absorption will not normally be an issue. In the next section we describe the calculation of the co-moving number density of globular clusters (GC) as a function of redshift for different evolutionary assumptions. In Section 3 we present the results of the number calculations. Section 4 considers the apparent sky clustering of the distant GC. We conclude with a discussion of the opportunities and complications that this population presents. The calculations are presented in a cosmology for which $H_0 = 70 \text{ km s}^{-1} \text{ Mpc}^{-1}$, $\Omega_M = 0.3$, $\Omega_\Lambda = 0.7$.

2. An Evolving Globular Cluster Luminosity Function

The expected sky density of GCs at magnitude m and redshift z depends on the product of the cosmological volume element and their luminosity function, $\phi_{GC}(L, z)$, integrated with the volume element along the line of sight. The luminosity function has three sources of

evolution. First, it is generally accepted that galactic tidal fields and stellar dynamical “shocks” erode a more numerous high redshift GC population into the remnant population we see today. We use the results of a relatively secure theoretical analysis of the evolution of the population, but also show results for a non-evolving distribution. Second, as the stellar population becomes younger with increasing redshift its spectral energy distribution changes. Third, the GCs form at some high, but as yet poorly determined, redshift. Our approach to each of these evolutionary terms along with the normalization to the present day globular cluster population is discussed in the following section.

2.1. An Evolving Mass Distribution

Recently Fall & Zhang (2001, hereafter referred to as FZ) have discussed a generalized dynamical model for the evolution of the mass distribution of GCs. They find that within 1-2 Gyr of origin, a wide range of initial GC mass distribution assumes a characteristic form which then evolves in a nearly self-similar way. At small mass, all clusters (in the same tidal field) go to zero mass at the same rate due to two-body relaxation driven evaporation. At high mass, gravitational shocks impose a characteristic maximum mass above which there is a rapid cutoff of numbers. The continual depletion of GCs implies that over a Hubble time about 10% of the initial cluster population survives, under the assumptions that the system is not replenished and that the galactic potential does not change. FZ have kindly made their results for the evolution of the globular cluster mass distribution available for use in this paper. Specifically we use the differential number of GCs at mass M at time t , $n_{GC}(M, t) dM$, which FZ present in their Figure 3.

It should be noted that the FZ model *predicts* the mass of the peak. To test this aspect of the models FZ have put the Milky Way globular clusters on a mass scale using $M/L_V = 3$, as is appropriate for an old, metal poor stellar population. The agreement between model and observation is impressively good. The extensive testing of FZ shows that the results should not change much with galaxy mass or galaxy type.

The FZ model results are specified at times of 0.01, 1.5, 3, 6 and 12 Gyr. We use a double spline function in the variable M and $\log t$ to interpolate to other times. We extrapolate slightly beyond their 12 Gyr model to the age of 13.4 Gyr age of our cosmology. The minimum age of their models is a 0.01 Gyr, where the “formation distribution” is close to a power law in mass. We will show the sensitivity of our results to the GC number evolution.

2.2. The Redshift Dependent Luminosity Function

We require the redshift dependent globular cluster luminosity function, $\phi_{GC}(L_{\bar{\lambda}}, z)$, where $L_{\bar{\lambda}}$ is the observed luminosity in some filter band centered around $\bar{\lambda}$. The conversion from $n_{GC}(M)$ to $\phi_{GC}(L)$ is made using a spectral synthesis model which gives the entire spectral energy distribution, F_{λ} , as a function of model age for given metallicity and star formation history. We use the PEGASE.2 code (Fioc & Rocca-Volmerange 1997) to calculate $\ell_{\bar{\lambda}}$, the observed frame luminosity per unit mass in the filter band $\bar{\lambda}$,

$$\ell_{\bar{\lambda}} = \frac{\int_0^{\infty} T(\lambda) F_{\lambda}((1+z)\lambda) d\lambda}{(1+z) \int_0^{\infty} T(\lambda) d\lambda}, \quad (1)$$

where $F_{\lambda}[(1+z)\lambda]/(1+z)$ is the model's mass normalized absolute flux in the observed frame and $T(\lambda)$ is the filter transmission function. Noting that the photon redshift and the time dilation are included in Eq. 1, an object of mass M gives an observed flux in the $\bar{\lambda}$ filter of

$$f_{\bar{\lambda}} = \frac{M\ell_{\bar{\lambda}}}{4\pi r^2(z)}, \quad (2)$$

where $r(z)$ is the co-moving distance in the adopted cosmology. The observed flux is converted to magnitudes using the definition $m_{\bar{\lambda}} \equiv -2.5 \log_{10}(f_{\bar{\lambda}}) + C$, where C is 31.4 AB magnitudes at 1 nano-Jansky.

2.3. Normalizing the Luminosity Function

The luminosity functions of the GC systems of the Milky Way and more than 50 nearby galaxies have been studied (Harris 1991; Harris 1996). A single galaxy's GC luminosity function is conventionally described as a Gaussian (in absolute magnitude, hence a lognormal distribution in luminosity) centered at $\langle M_V \rangle = -7.27 + 5 \log_{10}(H_0/75)$ mag with a dispersion of about 1.2 magnitudes. Although a more complex function, the FZ mass model appears to describe the data at least as well as a Gaussian. Moreover, it is based on a dynamical theory that allows its history to be predicted. To use the FZ function in our calculation we need to fix the volume normalization and we will also introduce a small shift in the M/L value.

2.3.1. Mass-Luminosity Normalization

The mass normalization of the FZ models is determined by the dynamics of the GCs within the model galaxy. Although fairly insensitive to variations in the potential, the mass

function does shift slightly depending on the specific galactic potential. Here we need the luminosity function typical of a mix of galaxies. We adopt the functional form of the FZ mass function and could adopt their $M/L_V = 3$ value, however we prefer to make a small adjustment to provide an alternate match to the observational data. The FZ mass function is a power law on the low mass side and much steeper than a Gaussian on the high mass side. Here we chose an M/L_V value that brings the mean luminosities of the FZ distribution to the mean of the Gaussian fits. A numerical integration finds that $M_V = -7.27$ mag should be identified as $\log M/M_\odot = 5.36$, which implies an $M/L_V = 3.3 M_\odot/L_\odot$. This small M/L change is well within the uncertainty of stellar population modeling. In particular, M/L_V is $2.1 M_\odot/L_\odot$ for the $Z = 0.1$ solar PEGASE models we compute at an age of 13.4 Gyr. Our normalization effectively raises the M/L values of the PEGASE models by a multiplicative factor of 1.57.

The V band luminosity is widely used to describe low redshift clusters. However, it is beneficial for the accuracy of our application to high redshift galaxies main application to use K band luminosities. Furthermore, the GC population is most closely connected to the old stellar population which is most accurately measured at low redshift by K band luminosities. The conversion from V to K must use the IR colors of a population with a metal abundance of about one-tenth solar, $V - K = 2.93 + 0.5Z/Z_\odot$ mag (Aaronson Cohen Mould & Malkan 1978). The $Z = 0.1Z_\odot$ PEGASE models find $V - K = 2.4$ mag at 13.4 Gyr which is in essentially exact agreement with the observational relation. Using this color we find that the mean peak K band luminosity for GCs is $\langle M_K \rangle = -9.70 + 5 \log_{10}(H_0/75)$. This value is converted to the flux based AB magnitude system with the addition of $AB(K) = +1.88$ mag.

2.3.2. Number Density Normalization

The mean co-moving density of GCs for a single galaxy is modeled as being directly proportional to its luminosity, (Harris & van den Bergh 1981; Harris 1991),

$$S_N = N_t 10^{-0.4(M_V + 15)}, \quad (3)$$

where M_V is the galaxy's absolute magnitude in the V band and N_t is the total number in a Gaussian luminosity function. The S_N relation has significant variations with Hubble type and possibly environment but appears to be accurate in the mean (Harris 1991). Since GC are most clearly associated with old stellar light it is natural to use a K band luminosity function, in which case,

$$S_N = N_t 10^{-0.4(M_K + 17.9)}, \quad (4)$$

where a galaxy with solar metallicity has $V - K \simeq 2.9$ mag (Aaronson Cohen Mould & Malkan 1978). Adopting the Gardner *et al.* (1993) luminosity function (for our purposes, similar to the recent Cole *et al.* 2001 results), for which $M_*(K) = -23.1$ mag, we find that in the K band the number of globular clusters around a galaxy rises linearly with luminosity,

$$N_t(L_K) = 120S_N \frac{L_K}{L_*(K)}. \quad (5)$$

To convert the normalization from globular cluster per galaxy to a volume normalization we use the luminosity density of galaxy light in the K band, $j(K)$. The normalizing constant for the GC luminosity function is defined such that the integral over all GC luminosities must be equal to the mean number of GC expected for the mean amount of galaxy light in that volume. That is,

$$\int_0^\infty \phi_{GC}(L_{\bar{\lambda}}, z = 0) dL = 120S_N \frac{j(K)}{L_*(K)}. \quad (6)$$

For Gardner’s (1993) $\alpha = -1$ Schechter luminosity function fit $j(K) = \phi_*(K)L_*(K)$, where $\phi_*(K) = 0.0166h^{-3} \text{ Mpc}^{-3}$. Note that the dependence on $L_*(K)$ cancels in Eq. 6. Then the co-moving volume density is GCs is $n_{GC}(0) = 2.0h^{-3}S_N \text{ Mpc}^{-3}$, where $h = H_0/100$. We adopt $S_N = 2$ as a reasonable and somewhat conservative value, given that the bulk of the K light emerges from relatively luminous early type galaxies. Figure 4 and Table 3 of Harris (1991) might suggest a value of about 3 for the early type galaxies, with evidence that strongly clustered early type galaxies have higher S_N . Of course the origin of these effects may well be directly visible in the future. The outcomes is that our complete GC luminosity function is,

$$\phi_{GC}(L_{\bar{\lambda}}, z) dL_{\bar{\lambda}} = n_{GC}(0)n_{GC}[L_{\bar{\lambda}}/\ell_{\bar{\lambda}}(t), t(z)] dL_{\bar{\lambda}}. \quad (7)$$

The redshift distribution per unit sky area of GC at a given flux level, is simply

$$n(z|f_{\bar{\lambda}}) d \ln f_{\bar{\lambda}} = \int_0^\infty \phi_{GC}(4\pi r^2(z)f_{\bar{\lambda}}, z) \frac{dV}{dz} dz d \ln f_{\bar{\lambda}}. \quad (8)$$

where dV/dz is the volume element within the model cosmology. Integrating over the redshift distribution gives the number-magnitude relation In practice, these calculations are done using magnitudes rather than fluxes.

3. Counts and Distributions

With the modeling apparatus in hand we first pause to show the low redshift $n(z)$ at $m_R(AB) = 25, 26, 27$ and 28 mag in Figure 1. The total sky densities of the FZ model at these

depths are 87, 321, 1,260 and 4,840 per square degree per magnitude, respectively. These GCs will be clearly associated with relatively bright galaxies, typically about $m_R(AB) = 13 - 17$ mag, with the redshift distributions shown.

3.1. Number Redshift Distributions

Precisely how globular clusters form is, at this time, unknown. Part of the point of this paper is that the plausible formation redshifts for the bulk of GCs will shortly come within reach of telescopes. To try to bracket the situation, we examine a number of somewhat extreme alternative models and look at the effects of co-ordinated bursts in a galaxy. To examine the importance of “luminosity spikes” at the time of formation, we use (arbitrarily, for the purpose of illustration) 10 bursts of star formation of duration 10 Myr spread over the 0 to 1 Gyr time interval. The formation age of all of the GC is put at 0.5 Gyr. The results are shown in Figure 2. Such bursts would only effect the counts in an area small enough that only a few dozen actively GC forming galaxies were present.

In Figure 3 we use the same set of ten star formation bursts but shifted in time to the 1 to 2 Gyr time interval with a uniform formation age of 1 Gyr. Clearly the bursts of star formation produce spikes in the redshift distribution but those effects quickly die away. It could be that the earliest phases of globular cluster formation are cloaked in dust which later disperses, following an age-extinction relation (Shapley et al. 2001). In that case the high luminosity peaks will be a briefly obscured phase in the life of GCs. However the Figures show that if those short-lived bright spikes are removed, neither the counts or redshift distribution will be greatly altered.

The difference between the no-evolution and FZ density evolution models are small at redshifts below about three, under the assumption that most globular clusters were formed at redshifts greater than three. The differences would be much larger if significant globular cluster formation continued to much lower redshift. The numbers predicted with a non-evolving mass model are nearly a full decade below the evolving model beyond redshifts of five. Since density and luminosity evolution are independent in these models the same difference applies to all formation histories.

3.2. Number Magnitude Relations

The number-magnitude relation is shown in Figure 4 in the V, R, J, K, L and M bands (spanning roughly 0.5 to 5 microns) for our model with ten, bursts of 10% of the mass, spread

between 0 and 1 Gyr. There are two effects. At low redshift the counts rise with increasing magnitude at a rate governed by the volume element, enhanced by k-corrections in an old, low metallicity, population. Although not shown, at 1 nJy in the V band the $n(z)$ peaks at about redshift 0.3. At 1 nJy in the R band $n(z)$ peaks at about redshift 0.5, with a few of the actively star-forming $z = 5$ clusters in formation being visible. Clearly deep optical band observations are not the ideal way to probe the formation epoch. The character of the redshift distribution changes in the infrared bands as the peak of the spectrum is redshifted into them. The combination of k-correction and luminosity evolution causes the counts in the redder bands to rapidly climb to several million per square degree. As Figure 4 shows, the counts are steeper than Euclidean near 30 AB mag in the IR bands.

The predicted counts for a wide range of model star formation histories are shown in Figure 5. We display the L band counts for models having ten bursts of 10% of the final mass star formation extending over 10 Myr in the 0-1 Gyr interval (triangles), the 1-2 Gyr interval (diamonds), and exponential models with $\tau = 1$ pentagons), 2 (heptagons) and 4 Gyr (hexagons) for both evolving and non-evolving mass function. The number-magnitude relation shows substantial model dependencies beginning at about 1 nJy ($m_{AB} = 31.4$ mag). However, the result that the L band counts will be around 10^8 per mag per square degree at 0.2 nJy is reasonably robust. It does not depend a lot on star formation, internal dust shrouding in the early phases, and is not unduly sensitive to the exact amount of GC density evolution. The biggest potential over-prediction of numbers is if GC initially form in dusty disk environments which makes them hard to detect. As long as the clusters become visible within about 2 Gyr of formation the numbers predicted here should be fairly accurate. The basic prediction that the sky density becomes about 10^7 per square degree around 1 nJy is difficult to escape, given the assumptions about globular cluster origins, evolution and visibility made in this paper.

4. Angular Clustering

Globular clusters are strongly concentrated around their host galaxies. At the very low flux levels we are investigating here it is natural to ask to what degree this clustering will remain evident and whether the nano-Jansky sky will effectively be covered with a nearly uniform distribution of GC. A prediction of clustering uses the results above but requires additional information about the degree to which galaxies and their GC systems merge into larger and larger units. Furthermore, the host galaxies may not always be visible at the highest redshifts considered here, since galaxies are generally younger and much lower surface brightness than GCs. Hence, the following estimates of galaxy-GC cross-correlations will be

upper limits, although we do incorporate a model for galaxy merging into our calculations.

The real space cross-correlation of galaxies and GCs can be derived from the average radial profile of GCs in their host galaxies. As shown below the auto-correlation of galaxies makes no significant contribution at the angles of interest. The FZ calculations find that after approximately 1 to 2 Gyr the radial distribution converges to a stable, nearly power-law form. An approximate power law fit to the Milky-Way data of Harris (1996) is,

$$n(r) = 3 \times 10^2 \left(\frac{r}{10\text{kpc}} \right)^{-3.5} \text{ kpc}^{-3}. \quad (9)$$

If there is a core in the radial distribution it appears at a radius of order a few kpc where the GCs become superimposed on significant galaxy light and hard to find. The Milky Way is probably somewhat less than L_* in luminosity and its GC system, with a total of 160 ± 20 clusters (Harris 1991), has numbers about 2/3 half of the 240 expected at L_* . To calculate the cross-correlation function with galaxies we need $\delta(r) = (n(r) - n_0)/n_0$, where n_0 is the mean density. We normalize these numbers to the volume average for L_* galaxies. The mean GC density of $4.0h^{-3}\text{Mpc}^{-3}$ we derived above becomes a physical density of $1.2 \times 10^{-8} \text{ kpc}^{-3}$ for $H_0 = 70$. Consequently we can re-express Eq. 9, as the over-density,

$$\delta(r) = 2.5 \times 10^{10} \left(\frac{r}{10\text{kpc}} \right)^{-3.5}. \quad (10)$$

Converting this to the standard correlation length form and using co-moving co-ordinates ($H_0 = 70$),

$$\xi_{gGC}(x) = \left(\frac{9.4\text{Mpc}}{x} \right)^{3.5} \frac{L_h}{L_*}, \quad (11)$$

where we have included the luminosity dependence, with L_h being the luminosity of the host galaxy. Note that an alternate description of this correlation length is $6.6h^{-1}\text{Mpc}$. In this calculation we have assumed that the low redshift S relationship holds in the earliest phases of the life of a galaxy which needs to be tested. An overall density normalization change has no effect on the correlations since the mean field density changes at the same rate, leaving δ invariant.

GC systems appear to always be associated with more or less virialized galaxies. They are not part of a clustering hierarchy that extends into the linear regime. Therefore we describe the over-density distribution as being fixed in physical co-ordinates. We therefore multiply Eq. 11 by the correlation function evolution term $(1+z)^\epsilon$. The quantity ϵ is equal to $\gamma - 3$ for fixed over-density in physical co-ordinates, as is appropriate here.

Galaxies are assembled over time through the merger process. A simple model for the increase of mass M is $dM/dt = \mathcal{R}(1+z)^{\mathcal{M}}$. Approximating $1+z = t_0/t$ (as in an empty

universe) this integrates to

$$M_0 - \mathcal{R}(\mathcal{M}t_0)^{-1}(1+z)^{\mathcal{M}-1}, \quad \mathcal{M} > 1, \quad (12)$$

$$M(z) = \begin{cases} & (13) \end{cases}$$

$$M_0 - \mathcal{R}t_0 \log(1+z), \quad \mathcal{M} = 1. \quad (14)$$

$$(15)$$

Note that $M(z)$ goes to zero for finite z for $\mathcal{M} > 1$. Reasonable values are $\mathcal{M} \simeq 1 - 3$ and $\mathcal{R}t_0 \simeq 0.2 - 0.5$ (Carlberg, et al. 2000; Le Fèvre et al. 2000). The resulting redshift dependent co-moving correlation function, $\xi_{gGC}(x|z)$, is,

$$\left(\frac{r_0(z)}{x}\right)^\gamma = (1+z)^\epsilon \left(\frac{r_{00}}{x(z)}\right)^\gamma \frac{M(z)}{M_0}. \quad (16)$$

The angular correlation function is simply related to the volume correlation through a projection over redshift,

$$\omega(\theta) = A(\gamma)\theta^{1-\gamma}N^{-2} \int n^2(z) \left(\frac{r_0(z)}{x}\right)^\gamma x \frac{H(z)}{c} dz, \quad (17)$$

where $N = \int n(z) dz$, $A(\gamma) = \Gamma(\frac{1}{2})\Gamma((\gamma-1)/2)/\Gamma(\gamma/2)$, and $H(z) = H_0[\Omega_M(1+z)^3 + \Omega_R(1+z)^2 + \Omega_\Lambda]^{1/2}$, with $\Omega_M + \Omega_R + \Omega_\Lambda = 1$.

We express the results as an angular correlation $\omega(\theta) = (\theta_0/\theta)^{\gamma-1}$. We evaluate the integral using the L band $n(z)$ at 1nJy. For our $r_{00} = 6.6h^{-1}$ Mpc Mpc, $\gamma = 3.5$, $\epsilon = 0.5$, we find $\theta_0 = 22$ and $18''$, with $\mathcal{R}t_0 = 0.5$ for $\mathcal{M} = 1$, and 2, respectively and 21 and $17''$ for $\mathcal{R}t_0 = 0.3$ for the same \mathcal{M} . Correlation angles of $20''$ correspond to physical distances of about 100 kpc around redshift three. Therefore the bulk of the GCs will be clearly associated with their host galaxies. The galaxies, if they exist and are not obscured, will be some $\sim 10 - 12$ mag brighter than the GCs, depending on the relative roles of merging and luminosity evolution. At $K_{AB} \simeq 20 - 22$ mag galaxies have mean sky separations of $\sim 20 - 40''$, so the sky will be effectively covered, albeit with a concentration toward galaxies, or, the still-dark halos that will become the sites of galaxies.

The GC-galaxy cross-correlation calculation ignores the contribution due to galaxy-galaxy clustering. The same of calculation shows that the much shallower $\gamma = 1.8$ of galaxy clustering the auto-correlation angle is about 2 arcsec, for $r_{00} = 5h^{-1}$ Mpc. For the GCs their steep cross-correlation with galaxies allows them to rapidly climb out of the projected distribution, which does not occur for the galaxy-galaxy correlation. The galaxy-galaxy contribution will only be visible at about an arc-minute, where the projected clustering

amplitude is only ~ 0.03 . At angles less than $20''$ the contribution is less than 10%, given our modelling for clustering. Of course globular cluster formation during merging is a special case.

5. Discussion and Conclusions

Globular clusters are, in the main, very old objects, likely formed in the first quartile of the age of the universe, implying strong luminosity evolution at high redshift. The combination of k-corrections and luminosity evolution put the bulk of their energy in the 3 to 5 micron bands. For a fairly wide range of density and luminosity evolution models there should be approximately 10^7 GC per square degree per magnitude, with a continuing steep rise in counts. In the optical bands the counts rise slowly with few GC appearing beyond redshift one.

Source confusion noise in flux and position measurements increases in proportion to the density of sources relative to the beam density, $(\ln 2/\pi)(D/\lambda)^2$ (Scheuer 1974; Condon 1974). The problems associated with confusion begin to arise when the source density is about $\sim 5\%$ of the beam density. Moreover the strong clustering of GC toward galaxies will create enhanced confusion in the neighborhood of galaxies. A diffraction limited 6m telescope operating at 4μ will have one source per beam (severe confusion) at a sky density 1.5×10^8 per square degree. For the relatively steep source counts found here and the high confidence detections that would be of interest to photometric redshift estimation techniques, the source density below about 1 nJy presents an issue to be carefully approached. In detail this problem could be more quantitatively addressed with simulated observations using the predicted counts. In a future paper we will also consider a more detailed model that incorporates dust and emission line nebula effects and a number of potential astrophysical complications.

The large density of high redshift GCs is both an opportunity and a challenge. In as much as GC are key indicators of how the extended low metallicity stellar halos of galaxies came into being, observations at nJy flux levels will directly probe their origins. On the other hand, the sky densities and flux levels are similar to those predicted for zero metallicity, “first light” objects. It will require some care to distinguish a young cluster of fairly normal stars with strong ionizing radiation from the unusual zero metallicity stars that are the first luminous objects. It will be fascinating to understand the relationship between these two “early light” populations.

I thank Mike Fall & Qing Zhang for providing the results of their mass evolution models. Mike’s comments also improved the presentation of the results. Chris Pritchett and Sidney

van den Bergh provided inspiration and comments on this subject. Research support from NSERC and CIAR are gratefully acknowledged.

REFERENCES

- Aaronson, M., Cohen, J. G., Mould, J., & Malkan, M. 1978, *ApJ*, 223, 824
- Ashman, K. M. & Zepf, S. E. 2001, *AJ*, 122, 1888
- Carlberg, R. G., and 13 colleagues 2000, *ApJ*, 532, L1
- Cen, R. 2001, *ApJ*, 560, 592
- Cole, S. et al. 2001, *MNRAS*, 326, 255
- Condon, J. J. 1974, *ApJ*, 188, 279
- Cote, P., Marzke, R. O., & West, M. J. 1998, *ApJ*, 501, 554
- Couchman, H. M. P. & Rees, M. J. 1986, *MNRAS*, 221, 53
- Fall, S. M. & Rees, M. J. 1977, *MNRAS*, 181, 73P
- Fall, S. M. & Zhang, Q. 2001, *ApJ*, 561, 751
- Fioc, M. & Rocca-Volmerange, B. 1997, *A&A*, 326, 950
- Gardner, J. P., Sharples, R. M., Frenk, C. S., & Carrasco, B. E. 1997, *ApJ*, 480, L99
- Haiman, Z. & Loeb, A. 1997, *ApJ*, 483, 21
- Haiman, Z., Abel, T., & Rees, M. J. 2000, *ApJ*, 534, 11
- Haiman, Z., Abel, T., & Madau, P. 2001, *ApJ*, 551, 599
- Harris, W. E. 1991, *ARA&A*, 29, 543-79
- Harris, W. E. 1996, *AJ*, 112, 1487
- Harris, W. E. & van den Bergh, S. 1981, *AJ*, 86, 1627
- Larsen, S., Brodie, J. P., Elmegreen, B. G., Efremov, Y. N., Hodge, P. W., & Richtler, T. 2001, *ApJ*, 556, 801
- Le Fèvre, O. et al. 2000, *MNRAS*, 311, 565

Searle, L. & Zinn, R. 1978, ApJ, 225, 357

Scheuer, P. A. G., 1974, MNRAS, 167, 329

Shapley, A. E., Steidel, C. C., Adelberger, K. L., Dickinson, M., Giavalisco, M., & Pettini, M. 2001, ApJ, 562, 95

VandenBerg, D. A. 2000, ApJS, 129, 315

van den Bergh, S. 1979, *in Scientific Research with the Space Telescope*, IAU Colloquium 54, ed. M. S. Longair and J. W. Warner, pp 151-161.

Zepf, S. E., Ashman, K. M., English, J., Freeman, K. C., & Sharples, R. M. 1999, AJ, 118, 752

Zhang, Q. & Fall, S. M. 1999, ApJ, 527, L81

Fig. 1.— The redshift distribution for $m_R(AB) = 25, 26, 27$ and 28 mag, comparing our evolving luminosity function (solid line) with its no-evolution form (dotted).

Fig. 2.— The redshift distribution in the L band (around 3.5 microns) where the GCs form over the time range of zero to one Gigayear in 10 bursts of 10Myr. The solid line is for the density evolution model the dotted line is for no density evolution. Curves are presented for 0.2, 0.5, 1, 2, 4, 10 and 20 nJy, equivalent to 33.15, 32.15, 31.4, 30.65, 29.9, 28.9 and 28.15 AB mag, respectively.

Fig. 3.— The redshift distribution in the L band for 10 bursts of 10Myr of GC formation over the 1 to 2 Gyr time interval. Line types are as in Fig. 2. The same magnitude limits as in Fig 2 are used.

Fig. 4.— The number per magnitude per square degree as a function of limiting AB magnitude for the V (triangles, orange), R (diamonds, light green), J (pentagons, green), K (hexagons, blue), L (heptagons, purple) and M (octagons, red) bands. The solid lines are evolving density models and the dotted for fixed co-moving density models.

Fig. 5.— The L band counts for cluster formation in the 0-1 Gyr interval (triangles, orange), the 1-2 Gyr interval (diamonds, light green), and exponential models with $\tau = 1$ Gyr (pentagons, green), 2 Gyr (hexagons, blue) and 4 Gyr (heptagons, purple) for both evolving and non-evolving mass functions.

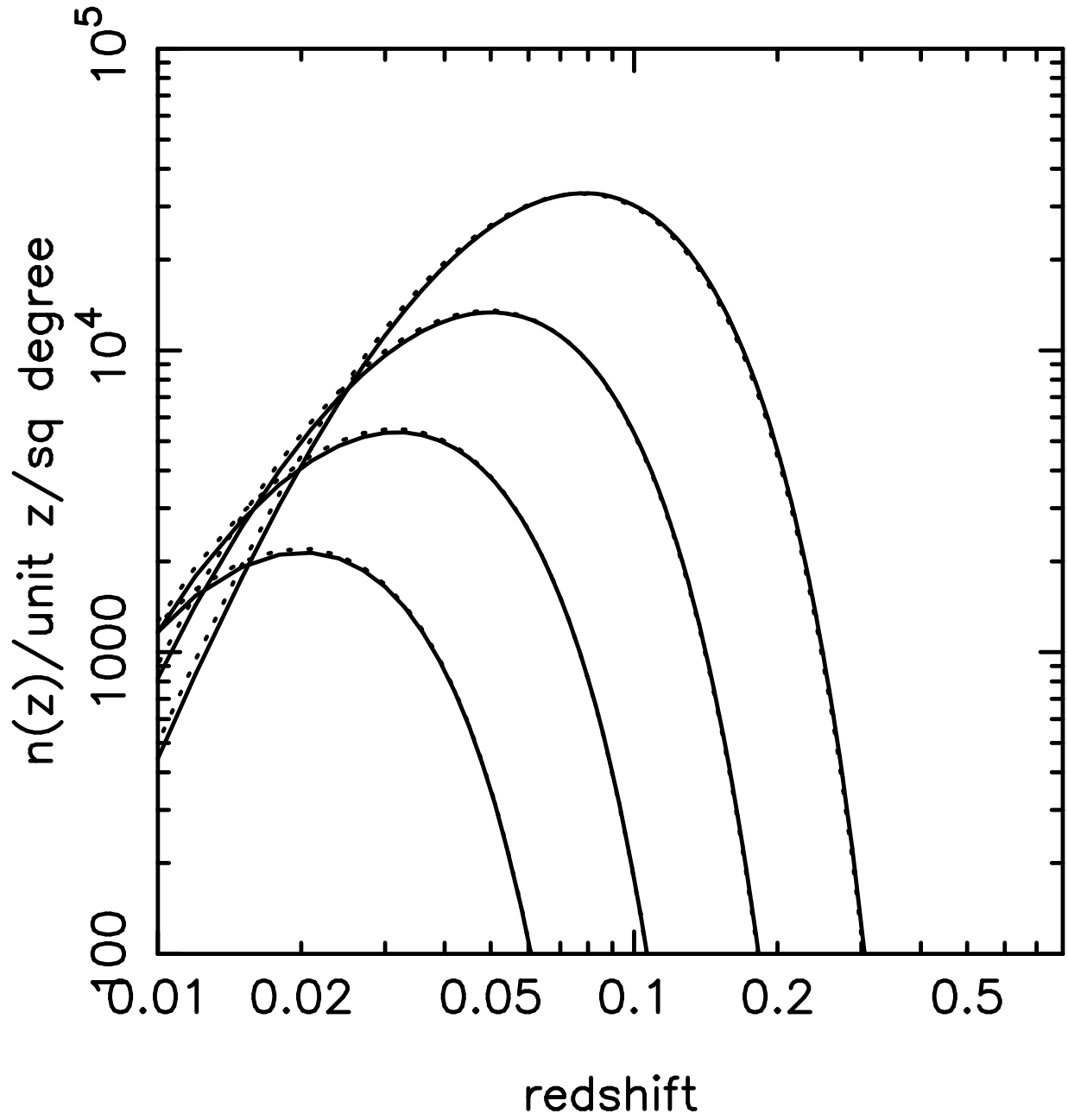


Fig. 1.—

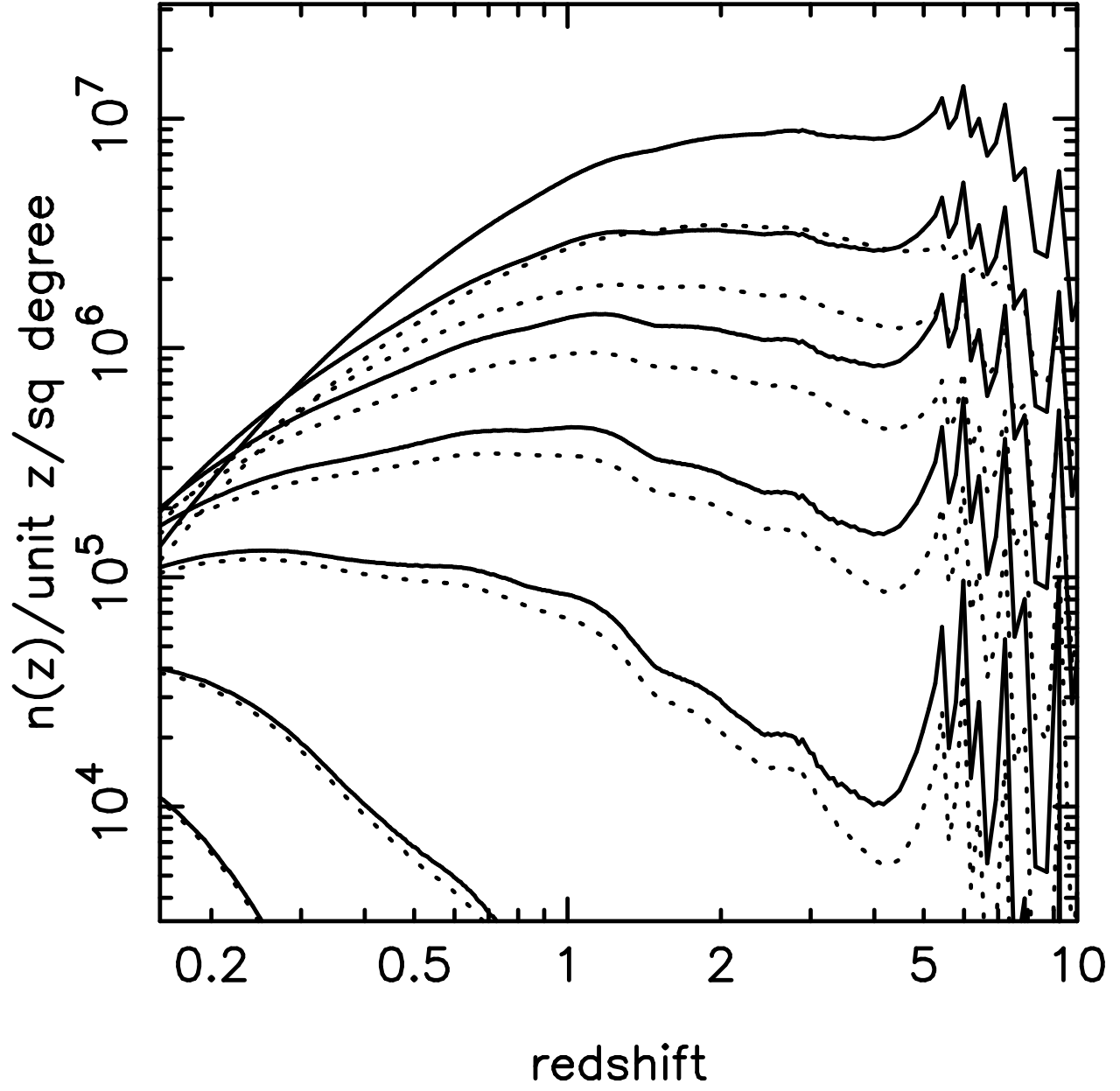


Fig. 2.—

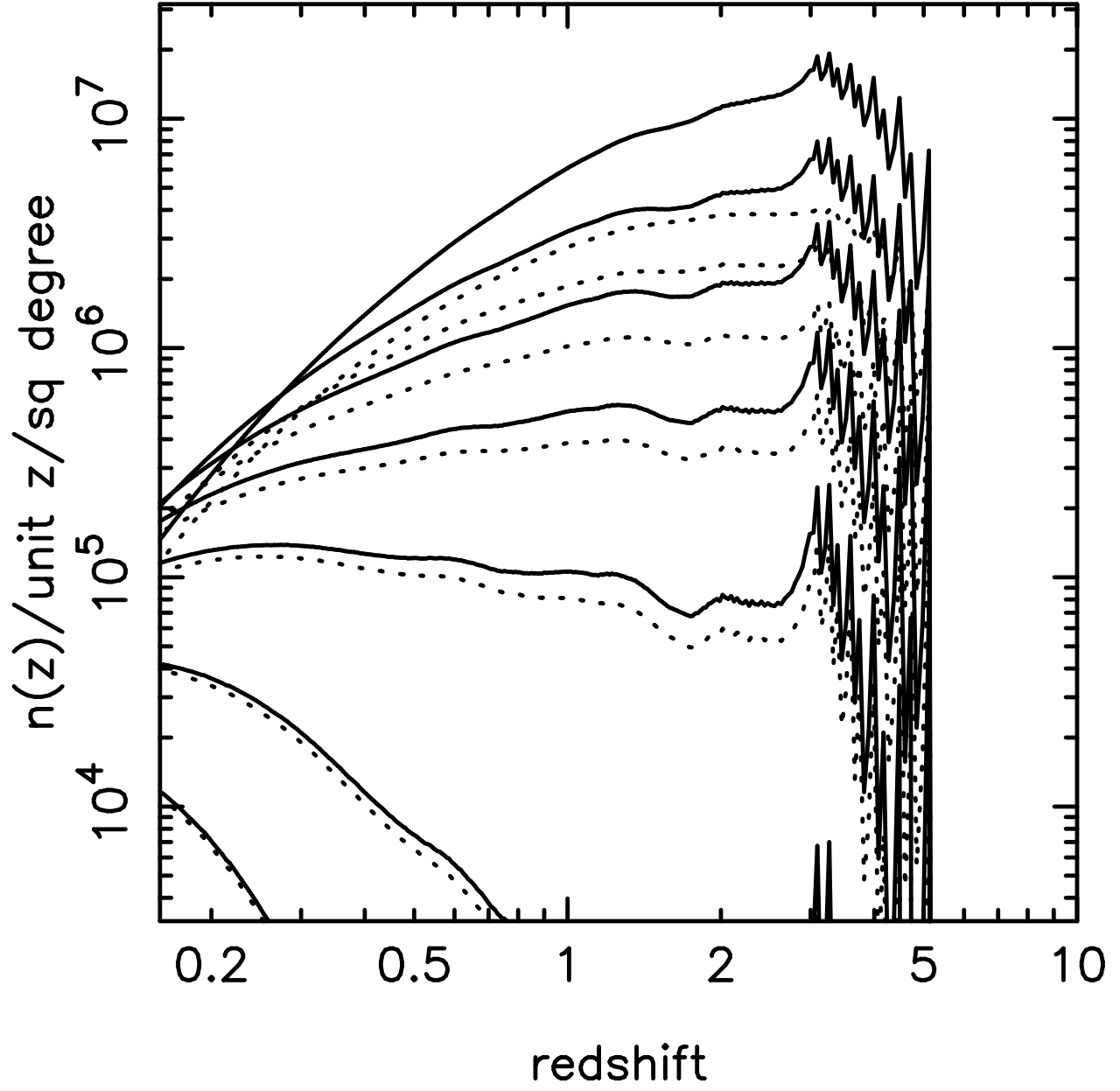


Fig. 3.—

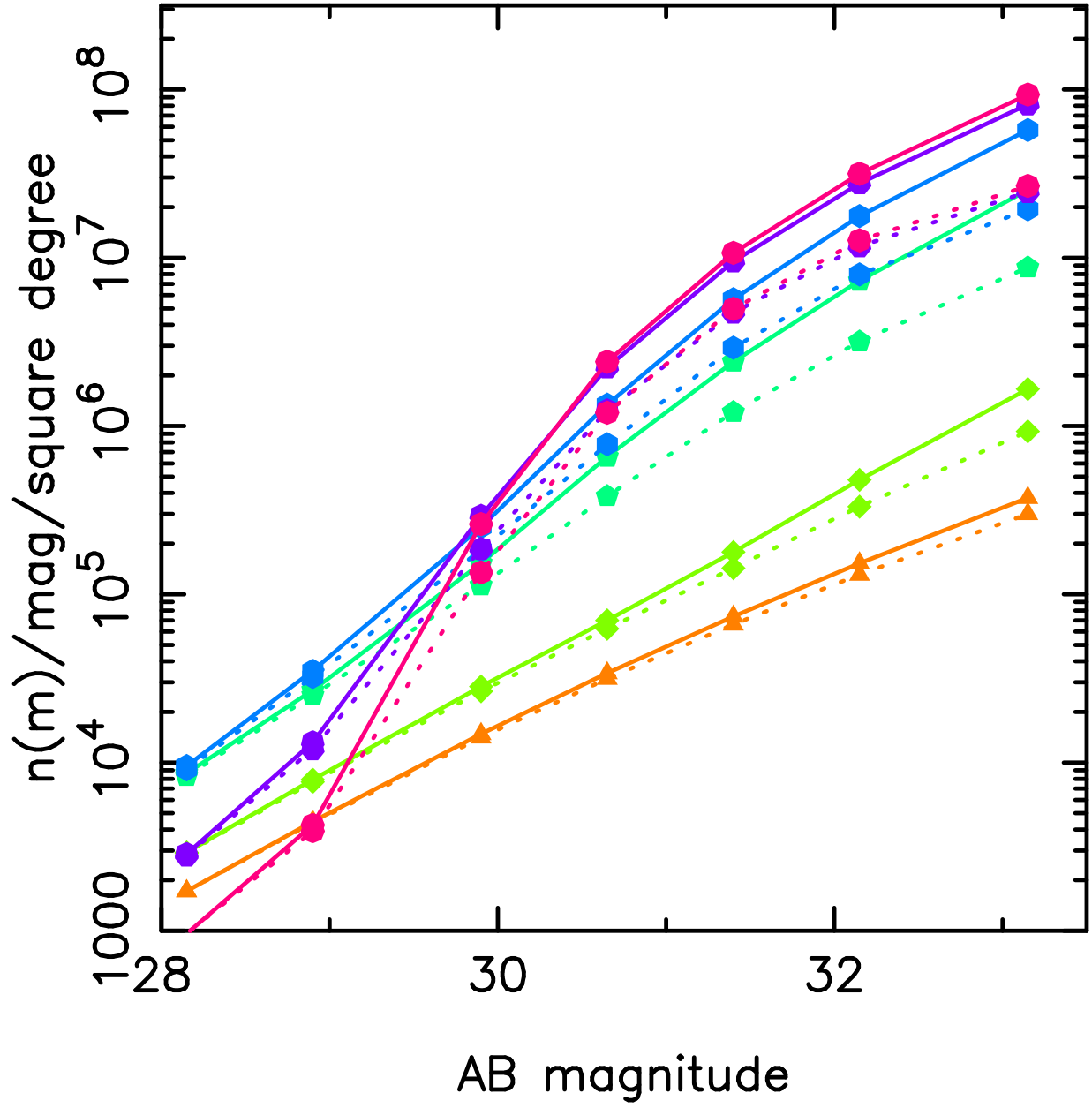


Fig. 4.—

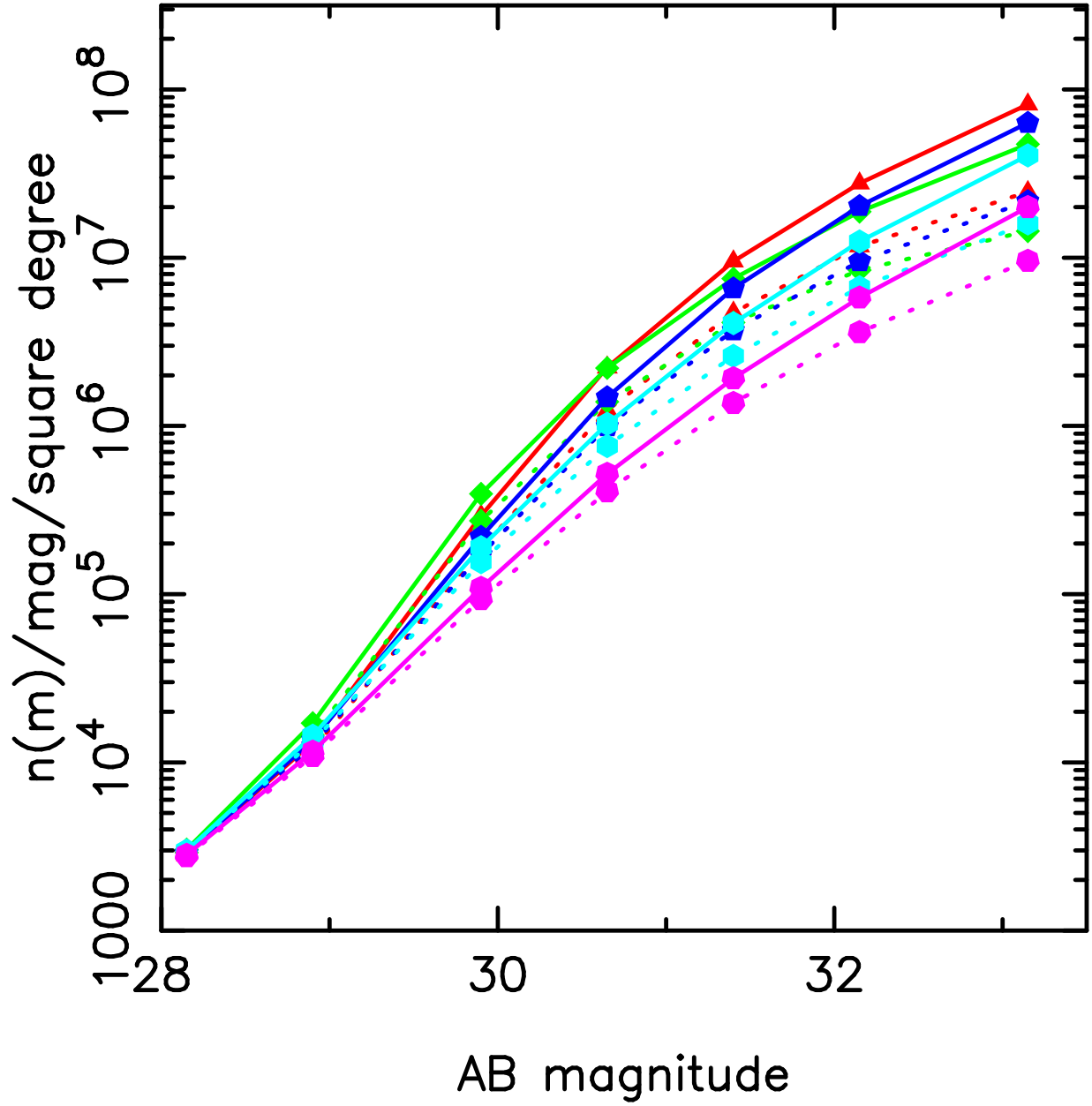


Fig. 5.—